Seismic design of buckling-restrained braced frames based on a modified energy-balance concept

Hyunhoon Choi, Jinkoo Kim, and Lan Chung

Abstract: The conventional energy-based seismic design procedure based on the energy-balance concept was revised for performance-based design of buckling-restrained braced frames. The errors associated with the energy-balance concept were identified and were corrected by implementing proper correction factors. The design process began with the computation of the input energy from a response spectrum. Then the plastic energy computed based on the modified energy-balance concept was distributed to each story and the cross-sectional area of each brace was computed in such a way that all the plastic energy was dissipated by the brace. The proposed procedure was applied to the design of three-, six-, and eight-story steel frames with buckling-restrained braces for three different performance targets. According to the time-history analysis results, the mean values of the top story displacements of the model structures, designed in accordance with the proposed procedure, corresponded well with the given target displacements.

Key words: energy-balance concept, buckling-restrained braces, hysteretic energy, performance-based seismic design.

Résumé : La procédure conventionnelle de conception antisismique basée sur l'énergie et fondée sur le concept d'équilibre énergétique a été révisée quant à la conception basée sur la performance des structures avec contreventements limitant le flambement. Les erreurs associées à ce concept d'équilibre énergétique ont été identifiées et corrigées en implantant des facteurs de correction appropriés. Le processus de conception a débuté par le calcul de l'intrant énergétique à partir du spectre de la réaction. Ensuite, l'énergie plastique calculée basée sur le concept modifié d'équilibre énergétique a été distribuée à chaque étage et la section de chaque contreventement a été calculée de manière à ce que l'énergie plastique soit entièrement dissipée par le contreventement. La procédure proposée a été appliquée à la conception de structures en acier à trois, six et huit étages munis de contreventements limitant le flambement pour trois comportements différents. Selon les résultats de l'analyse dans le temps, les valeurs moyennes des déplacements de l'étage supérieur des structures modélisées, conçues selon la procédure proposée, correspondaient bien aux déplacements ciblés donnés.

Mots clés : concept d'équilibre énergétique, contreventements limitant le flambement, énergie d'hystérèse, conception antisismique basée sur la performance.

Introduction

The energy-based seismic design methods, which utilize the hysteretic energy of a structure and the energy imparted to the structure during earthquake excitations, have been developed as potential alternatives to the conventional maximum value-based seismic design method. Since the concept of energy was introduced in seismic design by Housner (1956), a lot of effort has been made in the field of energy-based seismic engineering. Uang and Bertero (1988) compared the absolute and the relative energy and obtained story-wise distribution of hysteretic energy in multistory structures. Decanini and Mollaioli (2001) investigated the hysteretic energy to input energy ratio for various site conditions, hysteresis models, and ductilities. Estes and Anderson (2002) studied the hysteretic energy distribution over the height of structures using 40 earthquakes. That research was focused on the relationship between the energy imparted by earthquake and the energy dissipated in structures, and the characteratics of energy dissipation depending on design variables. Based on this research the reports *Performance-based seismic engineering of buildings* published by the Vision 2000 committee (SEAOC 1995) addressed the advantages and disadvantages of the energy-based seismic design as one of the performance-based seismic design methodologies. Since that time, studies on a detailed procedure for energy-based seismic design have progressed. Akbas et al. (2001) proposed a design procedure to dissipate input seismic energy by cumulative plastic rotation at the ends of beams. They assumed that the dissipated energy was distributed linearly along the building height. Leelataviwat et al. (2002) proposed a seismic-design method based on the energy-balance concept. Chou and Uang (2003) proposed a procedure to compute the total energy demand and to distribute it along the height of structures using inelastic energy spectra. Most of the above mentioned research was limited to design of moment-resisting frames.

Received 28 September 2005. Revision accepted 25 April 2006. Published on the NRC Research Press Web site at http://cjce.nrc.ca/ on 14 December 2006.

H. Choi. Department of Civil Engineering, University of Toronto, 35 St. George Street, Toronto, ON M5S 1A4, Canada.
J. Kim.[1] Department of Architectural Engineering, Sungkyunkwan University, 300 Cheoncheon-dong, Jangan-gu, Suwon, Gyeonggi-do, 440-746, Korea.
L. Chung. Department of Architectural Engineering, Dankook University, 147-Hannam-ro, Yongsan-gu, Seoul, 140-714, Korea.

Written discussion of this article is welcomed and will be received by the Editor until 28 February 2007.

[1]Corresponding author (e-mail: jkim12@skku.edu).

 doi: 10.1139/L06-068

The energy-balance concept, which provides a simple and convenient way for the energy-based seismic design of structures, is based on the assumption that the energy needed to push a structure up to the maximum target deformation is equal to the maximum earthquake input energy of an equivalent elastic system, which is further approximated by $mS_v^2/2$ (m is the mass and S_v is the pseudovelocity) (Housner 1956; Leelataviwat et al. 2002). The energy-balance concept was used to predict the maximum response of an inelastic system from the elastic reponse spectra for various target ductility ratios by Newmark and Hall (1982). Recently, Dasgupta et al. (2004) and Kim et al. (2005) applied the energy-balance concept for seismic design of buckling-restrained braced frames (BRBF). In both studies, the proposed design methods resulted in somewhat conservative design. The conservatism in design could also be found in the seismic design of moment frames utilizing the energy-balance concept (Leelataviwat et al. 2002). The reason can be found in the problems associated with the energy-balance concept and the energy-based seismic design such as: (*i*) the use of the pseudovelocity for estimation of the input seismic energy sometimes significantly underestimates the input energy demand (Uang and Bertero 1988); (*ii*) the input energy of an inelastic system is not equal to that of an equivalent elastic system (Fajfar and Vidic 1994; Dasgupta et al. 2004); and (*iii*) the plastic to input energy ratio estimated by the energy-balance concept is larger than the hysteretic energy to input energy ratio computed by time-history analysis.

In this study correction factors were derived first from a series of time history analyses to compensate for the inherent problems associated with the seismic design utilizing the energy-balance concept, and the modified energy-balance concept was applied to seismic design of steel frames with buckling-restrained braces (BRBs). Then the input energy was estimated from the response spectrum, and the plastic energy, modified to reflect the dissipated energy in structures during earthquake excitation, was distributed throughout the stories and the cross-sectional area of the BRB was obtained assuming that the energy imparted to each story was dissipated by the hysteretic behavior of the BRBs. The three-, six-, and eight-story framed structures with chevron-type BRBs were designed to meet given performance levels, and the results were verified through nonlinear time-history analyses.

Modification of the energy-balance concept

According to the energy-balance concept, the stored energy (E_i) of an equivalent elastic system, shown in Fig. 1, is equal to the energy combining the elastic energy (E_e) and the plastic energy (E_p) in the original elasto-plastic system at the maximum target displacement u_m. Housner (1956) also proposed that the maximum earthquake input energy of an equivalent elastic system be computed from the pseudo-velocity of an elastic response spectrum. These relationships can be expressed as follows:

$$[1] \qquad E_i = E_e + E_p$$

$$[2a] \qquad E_i = \frac{1}{2}u_e V_e = \frac{1}{2}mS_v^2$$

Fig. 1. Force-displacement relationship of an elasto-plastic and an equivalent elastic system.

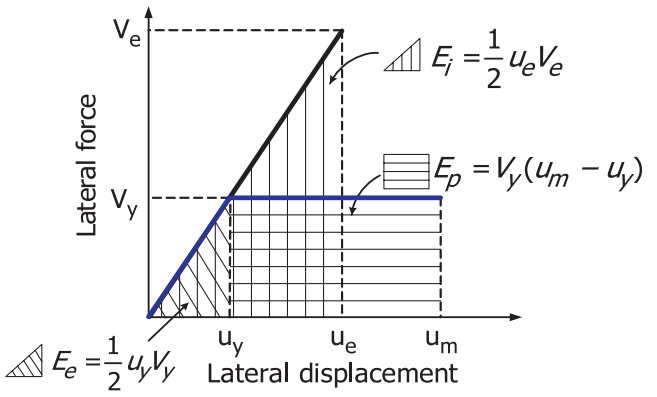

$$[2b] \qquad E_e = \frac{1}{2}u_y V_y$$

$$[2c] \qquad E_p = V_y(u_m - u_y)$$

where m is the mass of the system, S_v is the pseudo-velocity at the natural period of the system, and u_y is the displacement at yield. However, it needs to be pointed out that the energy balance or the equivalent energy concept is accurately applicable only to relatively short-period structures. For a structure with medium period, the so-called equal displacement concept, in which the maximum displacement of an inelastic system is equal to that of the equivalent elastic system, is generally applied.

In the following subsections, the validity of the basic assumptions of the energy-balance concept is investigated through time-history analysis of single-degree-of-freedom (SDOF) systems using 20 earthquake ground motions originally developed for the SAC steel project (Somerville et al. 1997). To construct the velocity and the energy spectra, the program code NONSPEC (Mahin and Lin 1983) was modified and used for the linear and nonlinear dynamic time-history analyses. The model structures analysed, the natural periods of which range from 0.05 to 3.0 s, have bi-linear force-displacement relationships with zero post-yield stiffness for nonlinear systems. Time-history analyses were carried out and the velocity and energy responses for the 20 earthquakes were averaged. The damping ratios of the model structures were assumed to be 5% of the critical damping.

Input seismic energy

Figure 2 plots the mean pseudo-velocities obtained from linear time-history analyses and the mean equivalent velocities obtained from the following equation:

$$[3] \qquad V_{eq} = \sqrt{\frac{2E_i}{m}}$$

where the maximum input energy, E_i, is obtained from linear time-history analysis. In Fig. 2, it can be observed that the mean values of the pseudo-velocity are significantly smaller than the mean equivalent velocity obtained from eq. [3], and consequently the input energy computed by eq. [2a] will underestimate the energy demand. Therefore, it can be concluded that the use of the pseudovelocity for estimation of the input

Fig. 2. Pseudo-velocity and equivalent velocity response spectra.

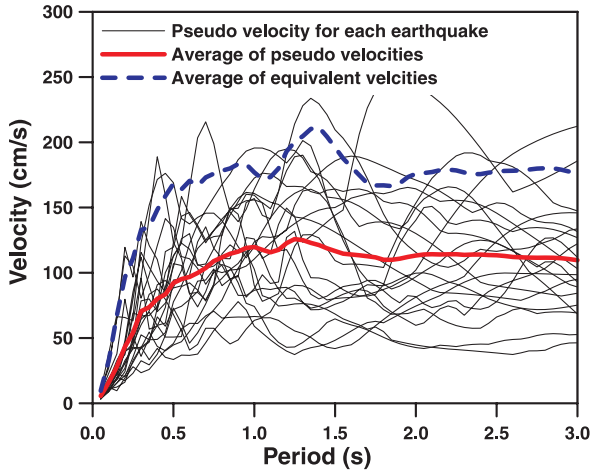

Fig. 3. Input energy spectra for various target ductility ratios.

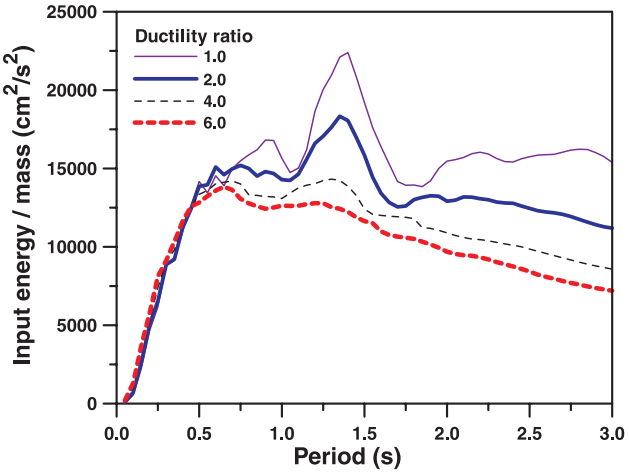

seismic energy can underestimate the input energy demand significantly.

Input energy in an inelastic and an equivalent elastic structure

As shown in Fig. 1 and eq. [1] the energy-balance concept is based on the assumption that the input energy in an equivalent elastic system is equal to that in an inelastic system. To investigate the validity of the assumption, time-history analyses of SDOF systems were carried out using the 20 seismic ground motions. Figure 3 depicts the seismic input-energy spectra for various target ductility ratios, which shows that the input energy in an inelastic system is close to that in the equivalent elastic system, in which the ductility is equal to one, when the natural period is less than about 0.45 s. In structures with the natural period larger than 0.45 s, however, the input energy in an inelastic system is considerably smaller than that in an equivalent elastic system. It can also be noticed that in those structures the input energy demand decreases as the target ductility ratio increases.

Plastic energy and hysteretic energy

Figure 4 shows the plastic energy to input energy ratios (E_p/E_i) estimated by the energy-balance concept and the hysteretic energy to input energy ratios (E_h/E_i) computed from time-history analysis. It can be observed that for a specific target ductility ratio, the plastic to input energy ratios are constant regardless of the natural period of the structures, and that the ratio increases as the target ductility ratio increases. On the other hand, the hysteretic energy to input energy ratios (E_h/E_i), obtained by time-history analyses, generally decrease as the natural period increases. The difference between energy ratios becomes smaller as the target ductility ratio becomes larger than six, probably due to the participation of damping energy, and the ratio E_h/E_i seems to increase only up to a certain value. This observation matches the findings of other researchers (Fajfar and Vidic 1994; Decanini and Mollaioli 2001; Khashaee et al. 2003). Therefore, it can be concluded that the plastic energy to input energy ratio estimated by the energy-balance concept is larger than the hysteretic energy to input energy ratio obtained by time-history analysis, and that the use of plastic energy in the energy-balance concept may considerably overestimate the

Fig. 4. Plastic energy to input energy ratio for various target ductility ratios.

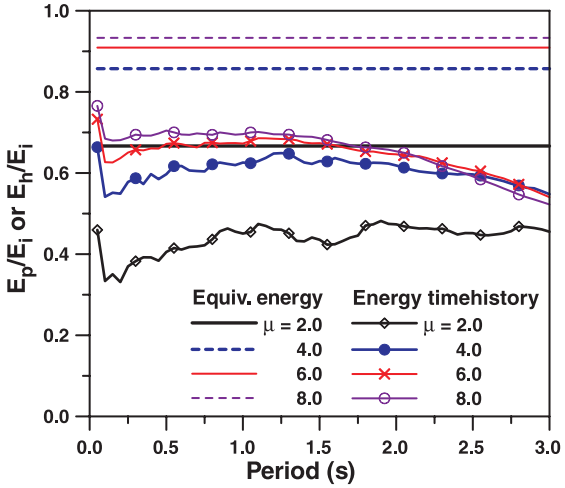

energy dissipated by the hysteretic behavior of structures during earthquake excitation.

Buckling-restrained braced frames

Buckling-restrained braces (BRBs) generally consist of a steel core undergoing significant inelastic deformation when subjected to strong earthquake loads and a steel casing for restraining global and local buckling of the core element (Fig. 5). A series of experiments by other researchers (Black et al. 2002; Merritt et al. 2003), proved a stable hysteretic behavior and high ductility capacity. Therefore, the use of BRBs greatly increases the energy dissipation capacity of the system and decreases the demand for inelastic deformation of the other structural members.

If a BRB is placed as a diagonal member with the slope θ as shown in Fig. 6, the energy (E_{pb}) dissipated by the BRB in one cycle of vibration is four times the plastic energy when it is deformed to the maximum displacement, which corresponds to the area of the hatched rectangle in Fig. 7

Fig. 5. Buckling-restrained braces (Clark et al. 1999).

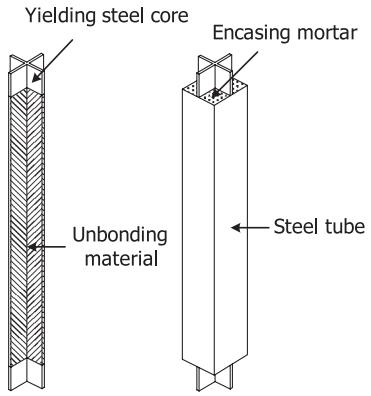

Fig. 6. Deformed configuration of buckling-restrained braced frame.

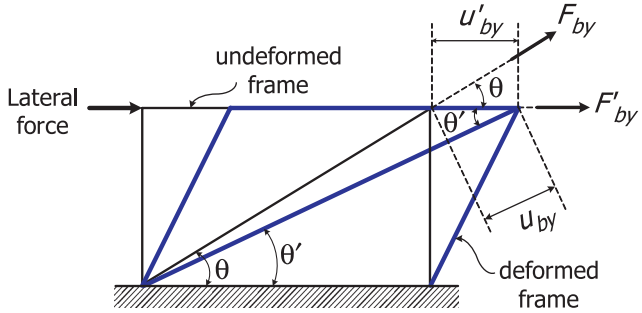

$$[4] \quad E_{pb} = 4F'_{by}(u_{bm} - u'_{by}) = 4A_b\sigma_{by}\cos\theta\left(u_{bm} - \frac{L_b\sigma_{by}}{E_b\cos\theta}\right)$$

where F'_{by} is the yield force ($= F_{by}\cos\theta = A_b\sigma_{by}\cos\theta$); u'_{by} is the lateral yield displacement ($= \frac{u_{by}}{\cos\theta} = \frac{1}{\cos\theta}\frac{L_b}{E_b}\sigma_{by}$); A_b, L_b, and θ are the cross-sectional area, length, and slope of the BRB, respectively; and E_b is the elastic modulus of the BRB. In the derivation of the above equation, it is assumed that the BRB has an elastic-perfectly plastic force-deformation relationship.

Design procedure

In this section, the proposed procedure for performance-based seismic design of a buckling-restrained braced frame (BRBF) is summarized. The procedure is considered to be an improvement of the design method proposed previously by the authors (Kim et al. 2005) taking the observation presented in Sect. 2 into consideration; i.e., the input energy and plastic energy obtained using the energy-balance concept is corrected in each step of the design procedure. Basically, the gravity load-resisting system consisting of pin-connected beams and columns is designed to remain elastic, and the BRB is designed to dissipate all the seismic input energy.

Step 1. Determination of yield displacement

Once the geometry and yield stress of the BRB are determined, the yield displacement (u'_{byi}) in each story of the BRBF

Fig. 7. Plastic energy stored in a buckling-restrained brace.

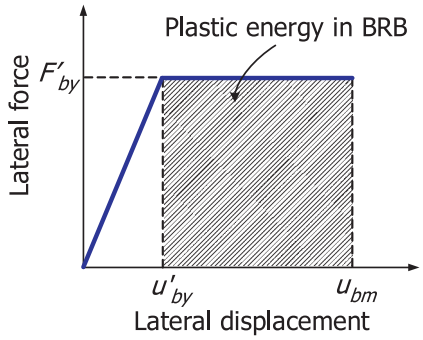

can be derived as follows (Fig. 6)

$$[5] \quad u'_{byi} = \frac{\sigma_{byi}L_{bi}}{E_b\cos\theta_i}$$

where σ_{byi}, L_{bi}, and θ_i are the yield stress, length, and the slope of the brace in the ith story, respectively. If the story heights and the yield stress of braces are the same throughout the stories, the roof displacement of the structure at yield, u_y, is the story yield displacement multiplied by the number of stories, N

$$[6] \quad u_y = \sum_{i=1}^{N} u'_{byi} = \left(\frac{\sigma_{by}L_b}{E_b\cos\theta}\right)N$$

For multistory structures the yield displacement (u_y) and the given target displacement (u_T) are converted to those of the equivalent SDOF system using the following equations (ATC 1996):

$$[7] \quad u_{T\,eq} = \frac{u_T}{\Gamma_1\phi_{t1}}, \qquad u_{y\,eq} = \frac{u_y}{\Gamma_1\phi_{t1}}$$

where Γ_1 and ϕ_{t1} are the modal participation factor and the roof story component of the fundamental mode shape vector, respectively. In the first stage, the fundamental mode shape can be assumed to be linear. With the yield displacement computed from eqs. [6] and [7], the predetermined target displacement and the target ductility ratio can also be computed, which will be used later to obtain the correction factors.

Step 2. Estimation of input energy (E_i^*)

To obtain the input energy using the energy-balance concept, the original multiple degrees of freedom (MDOF) structure needs to be transformed into an equivalent single degree of freedom (SDOF) system. Then the seismic input energy is estimated from eq. [2a] which is rewritten as follows:

$$[8] \quad E_i = \frac{1}{2}M_1S_v^2 = \frac{1}{2}M_1\left(\frac{T_1S_a}{2\pi}\right)^2$$

where M_1 is the first modal mass; S_v and S_a are the pseudo-velocity and pseudo-acceleration corresponding to the first natural period of the structure, T_1. In the first stage of design the natural period needs to be assumed; once the first-trial value for the cross-sectional area of the BRB is determined, the natural period can be computed more rigorously using an eigenvalue analysis. In this study, the first trial value for the natural period

is computed using the IBC-2000 formula for concentric braced frame (ICC 2000)

$$[9] \qquad T_1 = 0.0488h^{3/4}$$

It was shown previously that the use of eq. [8] underestimates the seismic energy imparted by an earthquake excitation significantly. It was also illustrated that the input energies in an elastic and in an inelastic structure are not the same. Based on these observations a modification factor α was introduced to obtain the modified input energy E_i^*

$$[10] \qquad E_i^* = \alpha E_i, \qquad \alpha = \left(\frac{E_{i,inelastic}}{E_{i,elastic}}\right)\left(\frac{V_{eq}}{S_v}\right)^2$$

Step 3. Estimation of the yield base shear (V_y)

The yield base shear can be estimated as follows using eqs. [1] and [2]:

$$[11] \qquad \begin{aligned} E_i^* &= E_e + E_p \\ &= \frac{1}{2}V_y u_{y\,eq} + V_y(u_{T\,eq} - u_{y\,eq}) \\ &= V_y\left(u_{T\,eq} - \frac{1}{2}u_{y\,eq}\right) \\ &= V_y u_{T\,eq}\left(1 - \frac{1}{2\mu}\right) \end{aligned}$$

$$[12] \qquad V_y = \frac{E_i^*}{u_{T\,eq}\left(1 - \frac{1}{2\mu}\right)}$$

where the target ductility ratio, μ, is expressed as $u_{T\,eq}/u_{y\,eq}$.

Step 4. Estimation of the total plastic energy (E_{pM}^*)

The elastic energy, E_e, can be obtained by substituting the yield base shear estimated in Step 3 into eq. [2b]. The plastic energy is the remaining energy after subtracting the elastic energy from the input energy, E_i^*. However as the plastic energy to input energy ratio (E_p/E_i) estimated by the energy-balance concept generally overestimates the actual hysteretic energy ratio, the plastic energy is modified by being multiplied by the correction factor β:

$$[13] \qquad E_p^* = \beta(E_i^* - E_e), \qquad \beta = \frac{E_h/E_i}{E_p/E_i}$$

In addition, the plastic energy of an equivalent SDOF system needs to be converted into that of the original multistory structure, E_{pM}^*

$$[14] \qquad E_{pM}^* = \gamma E_p^*, \qquad \gamma = \frac{E_{p,MDOF}}{E_{p,ESDOF}}$$

Step 5. Story-wise distribution of plastic energy

The plastic energy, E_{pM}^*, obtained above is distributed throughout the stories, and the BRBs are designed in such a way that all the plastic energy is dissipated by the BRBs. Therefore, proper distribution of plastic energy is necessary so that the plastic deformation in a BRB is not concentrated in a few stories and the performance of each brace is maximized. Estes and Anderson (2002) found that the hysteretic energy demand in each story of steel moment frames is largest in the first story and decreases linearly in higher stories. Akbas et al. (2001) assumed linear distribution of hysteretic energy in an energy-based design of steel frames. In this study, the story-wise distribution patterns for hysteretic energy were obtained through nonlinear time-history analyses.

Step 6. Determination of the cross-sectional area of the buckling-restrained braces in each story

The cross-sectional area of the BRBs in the ith story, A_{bi}, required to dissipate the specified input energy is determined by equating the plastic energy demand in the ith story, E_{pMi}^*, to the plastic energy stored in the BRB when it is deformed to the target displacement

$$[15] \qquad A_{bi} = \frac{E_{pMi}^*}{4\sigma_{by}\cos\theta_i\left(u_{bT} - \frac{L_{bi}\sigma_{by}}{E_b\cos\theta_i}\right)}$$

where u_{bT} is the maximum lateral displacement of a BRB corresponding to the target displacement of the story. The first-trial values for the plastic energy and BRB size are obtained based on the assumed natural period and mode-shape vector, and later more accurate values for these quantities can be obtained by eigenvalue analysis using the first-trial size of the BRBs. The size of a BRB is refined using the newly obtained natural period and mode-shape vector, and this process is repeated until convergence. Two or three iterations are generally required to reach the converged value of the BRB size.

Applicaton of the proposed design procedure

Model structures and earthquake loads

The three-bay and three-, six-, and eight-story framed structures with chevron-type BRBs were prepared for application of the proposed design method. The bay length of the model structures is 7.3 m and the height of the story is 5.5 m in the first story and is 3.7 m in the other stories. The weight of each story is 1538 kN and the inherent modal-damping ratios are assumed to be 5% of the critical damping. The member cross-sectional dimensions of the model structures are presented in Fig. 8. The 20 earthquake records, used previously in Sect. 2, were used again to design the structures, to obtain the correction factors, and to check whether the maximum displacements satisfy the given target displacements. The response spectra of the 20 records are plotted in Fig. 9 along with their mean spectrum, which show that the earthquake records have quite different frequency contents.

Story-wise energy distribution

To determine the appropriate size of the BRB using the proposed procedure, the story-wise energy distribution of the input energy needs be provided. According to analysis results of Choi and Kim (2006), no discernable difference could be observed in the displacement responses between the story-wise hysteretic energy distribution pattern computed from dynamic analysis and the simplified triangular distribution form. In this study,

Fig. 8. Model structures with buckling-restrained braces: (*a*) a three-story structure, (*b*) a six-story structure, and (*c*) an eight-story structure.

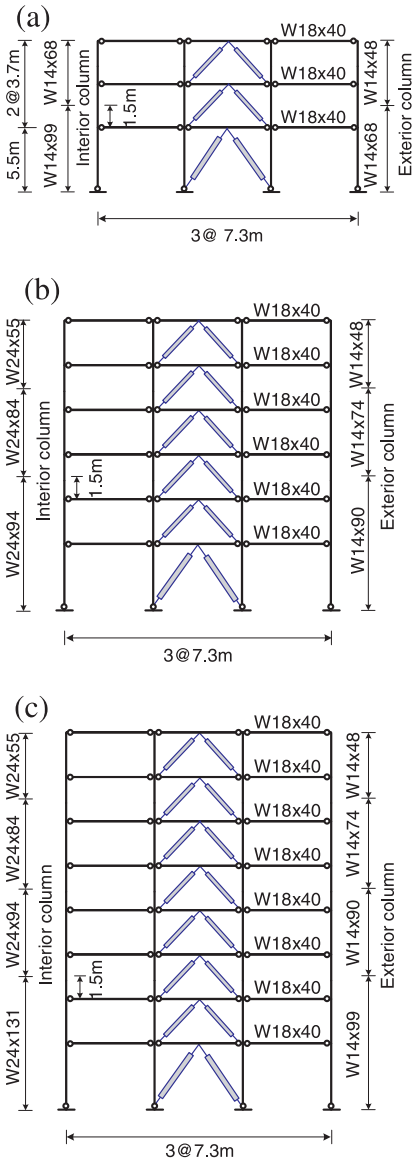

however, nonlinear time-history analysis was carried out using the program code Drain-2D+ (Tsai and Li 1997) to establish the story-wise energy distribution. In the analysis, the preliminary size of the BRBs was determined using the conventional strength design method presented in the IBC-2000. It was assumed that the post-yield stiffness of the beams and columns was 2% of the initial stiffness and that the force-deformation relationship of a BRB was bilinear both in tension and compression with zero post-yield stiffness. Figure 10 shows the hysteretic energy demand in each story normalized by that of the first story. After the story-wise energy distribution patterns were obtained, the original structures were transformed into the equivalent SDOF systems to use the energy-balance concept. The ratio of hysteretic energy in the original and the equivalent SDOF structures (γ) are plotted in Fig. 11.

Fig. 9. Acceleration response spectra of earthquake records used in the analyses.

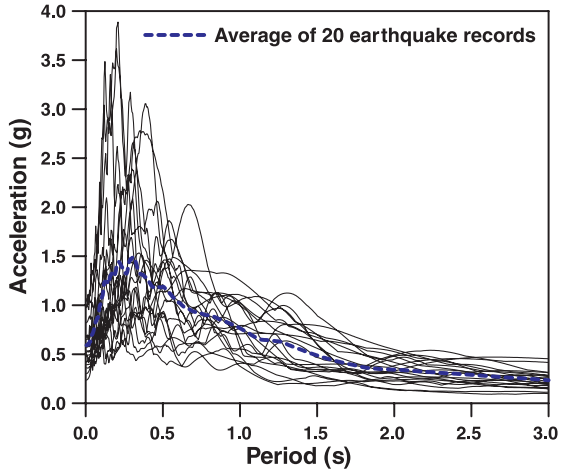

Design of buckling-restrained braces to meet a target displacement

The proposed design procedure was applied to determine the appropriate size of tthe BRBs to meet a given target displacement. The target displacements were set to be 1.0%, 1.5%, and 2.0% of the structure heights in all model structures. The yield displacement for a given target displacement was computed first, and from the target and yield displacements the ductility demand was obtained to compute the correction factors for the input and the plastic energies. Once the correction factors are prepared for various natural periods, they can be used repeatedly in the iteration process. The proposed design procedure for the three-story model structure (Fig. 8*a*) with 1.5% target displacement is summarized in the following.

Step 1. Determination of the yield displacement and the ductility demand

The target displacement at the top story is 19.2 cm and the yield displacement is computed from eq. [6] as follows:

$$u_y = \sum_{i=1}^{3} \frac{\sigma_{by} L_{bi}}{E_b \cos\theta_i}$$

$$= \frac{9.8\ \text{kN/cm}^2 \times 659.4\ \text{cm}}{19994.8\ \text{kN/cm}^2 \times 0.5547} + 2\left(\frac{9.8\ \text{kN/cm}^2 \times 517.3\ \text{cm}}{19994.8\ \text{kN/cm}^2 \times 0.7071}\right)$$

$$= 1.301\ \text{cm}$$

The displacement ductility, which is the target displacement divided by the yield displacement, is computed as 14.8. The first modal mass, the modal participation factor, and the roof story component of the normalized fundamental mode shape vector are 4.25 kN·s^2/cm, 1.265, and 1.0, respectively. From eq. [7] the target and the yield displacements of the equivalent SDOF system are computed as follows:

Fig. 10. Story-wise hysteretic energy distribution ratio: (*a*) a three-story structure, (*b*) a six-story structure, and (*c*) an eight-story structure.

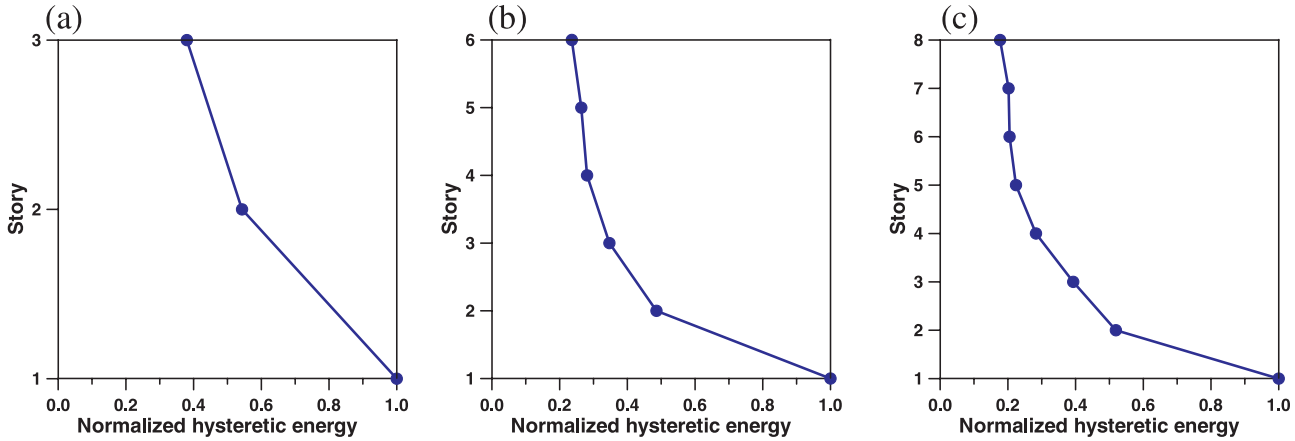

Fig. 11. Energy ratios of original and equivalent single-degree-of-freedom structures (γ).

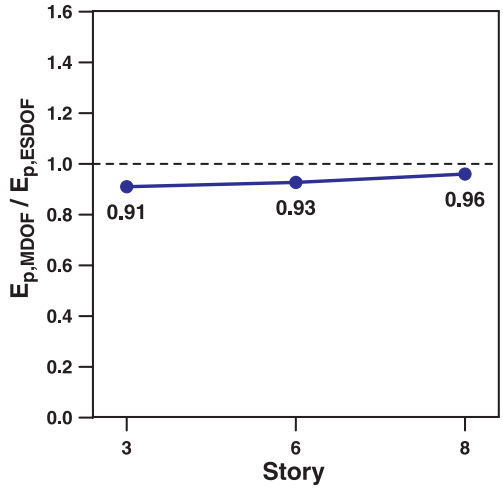

$$u_{\text{Teq}} = \frac{u_{\text{T}}}{\Gamma_1 \phi_{\text{t1}}} = \frac{19.202\ \text{cm}}{1.265 \times 1.0} = 15.179\ \text{cm}$$

$$u_{\text{yeq}} = \frac{u_{\text{y}}}{\Gamma_1 \phi_{\text{t1}}} = \frac{1.301\ \text{cm}}{1.265 \times 1.0} = 1.0285\ \text{cm}$$

Step 2. Estimation of the input energy (E_{i}^*)

The first trial period is computed as $0.0488(12.8)^{3/4} = 0.33$ s. It can be observed in the mean-response spectrum plotted in Fig. 12 that the pseudo-acceleration corresponding to this period is $+1.35g$. In the next stage, the input energy can be computed using the pseudo-acceleration and eq. [8]. This input energy should be modified by the factor α (eq. [10]), which is composed of the ratios $V_{\text{eq}}/S_{\text{v}}$ and $E_{\text{i,inelastic}}/E_{\text{i,elastic}}$. The two quantities are plotted in Figs. 13 and 14, respectively. With the first trial values of the natural period and target ductility, the modified input energy is determined as follows:

$$E_{\text{i}}^* = \left(\frac{E_{\text{i,inelastic}}}{E_{\text{i,elastic}}}\right)\left(\frac{V_{\text{eq}}}{S_{\text{v}}}\right)^2 E_{\text{i}}$$
$$= 1.175 \times 1.84^2 \times 10245.1\ \text{kN·cm}$$
$$= 40592.8\ \text{kN·cm}$$

Fig. 12. Accelerations determined in each trial.

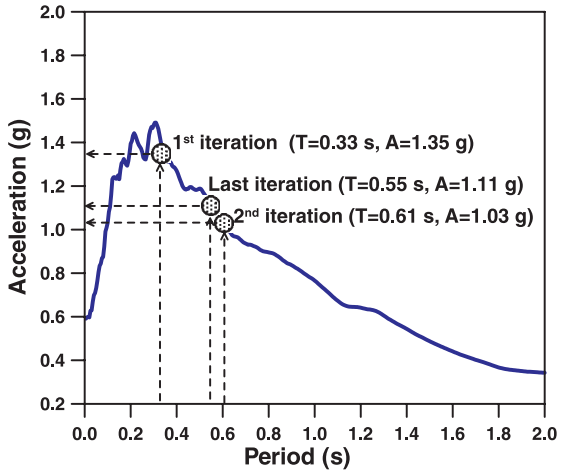

Step 3. Estimation of the yield base shear (V_{y})

The design base shear of 2768 kN is obtained by substituting the input energy and the ductility demand into eq. [12].

Step 4. Estimation of the total plastic energy (E_{pM}^*)

The elastic energy stored in the equivalent SDOF system is calculated as

$$E_{\text{e}} = \frac{1}{2} u_{\text{yeq}}\ V_{\text{y}}$$
$$= \frac{1}{2} \times \frac{u_{\text{y}}}{\Gamma_1}\ V_{\text{y}}$$
$$= \frac{1}{2} \times \frac{1.301\ \text{cm}}{1.265} \times 2768\ \text{kN}$$
$$= 1423.3\ \text{kN·cm}$$

After subtracting the elastic energy from the input energy, the plastic energy of the original structure can be obtained considering the ratio of the plastic energy to the input energy, β, and the ratio of the plastic energy of SDOF and MDOF systems, γ. The correction factors β and γ are obtained from Figs. 15 and 12, respectively, with a ductility demand of 14.8.

Table 2. Final values for the BRB cross-sectional area (cm^2).

Story	3			6			8		
Target displacement ratio (%)	1.0	1.5	2.0	1.0	1.5	2.0	1.0	1.5	2.0
μ	9.8	14.8	19.7	10.0	15.0	20.0	10.0	15.1	20.1
Period (s)	0.441	0.546	0.658	0.848	1.090	1.361	1.140	1.561	2.645
A_{b8}	—	—	—	—	—	—	23.2	11.1	3.6
A_{b7}	—	—	—	—	—	—	26.5	12.7	4.1
A_{b6}	—	—	—	28.0	15.9	9.9	26.9	12.9	4.1
A_{b5}	—	—	—	31.3	17.8	11.0	29.4	14.1	4.5
A_{b4}	—	—	—	33.4	18.9	11.7	37.1	17.8	5.7
A_{b3}	35.6	23.2	15.9	41.2	23.4	14.5	51.6	24.8	7.9
A_{b2}	50.9	33.1	22.8	57.7	32.7	20.3	68.1	32.7	10.5
A_{b1}	80.5	52.2	35.8	101.8	57.5	35.6	112.5	53.8	17.2

Fig. 13. Ratio of the equivalent velocity and the pseudo-velocity.

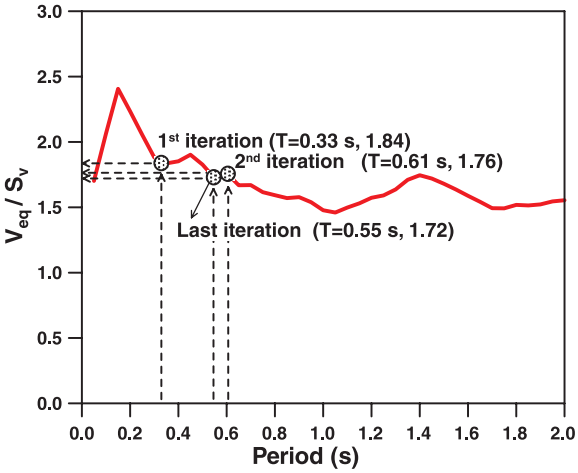

Fig. 14. Input energy ratio of the inelastic and elastic systems ($\mu = 14.8$).

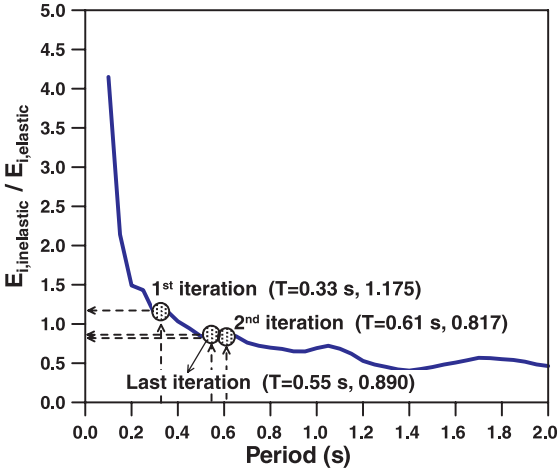

$$E^*_{pM} = \gamma\beta E_p = \left(\frac{E_{p,MDOF}}{E_{p,ESDOF}}\right)\left(\frac{E_h/E_i}{E_p/E_i}\right)E_p$$
$$= 0.91 \times 0.757 \times 39169.4 \text{ kN·cm}$$
$$= 26981.1 \text{ kN·cm}$$

Fig. 15. Plastic energy to input energy ratio (β) for $\mu = 14.8$.

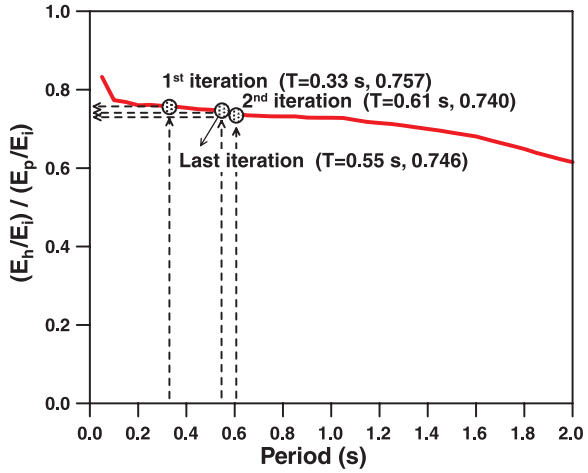

Table 1. Process of determining the BRB cross-sectional area in the three-story structure for 1.5% target displacement.

Trial	1	2	…	Final
Period (s)	0.330	0.607	…	0.546
Acceleration (g)	1.347	1.033	…	1.109
V_{eq}/S_v	1.836	1.761	…	1.723
$E_{i,inelastic}/E_{i,elastic}$	1.175	0.817	…	0.890
E_i^* (kN·cm)	40 592.8	52 472.2	…	50 970.2
V_y (kN)	2768.0	3532.6	…	3428.5
$(E_h/E_i)/(E_p/E_i)$	0.757	0.740	…	0.746
$E_{p,MDOF}/E_{p,ESDOF}$	0.91	0.91	…	0.91
E^*_{pM} (kN·cm)	26 981.1	34 072.8	…	33 374.8
A_{b3} (cm^2)	18.7	23.7	…	23.2
A_{b2} (cm^2)	26.8	33.8	…	33.1
A_{b1} (cm^2)	42.2	53.2	…	52.2

Step 5. Story-wise distribution of plastic energy

Total plastic energy (E^*_{pM}) estimated in Step 4 is distributed throughout the stories according to the story-wise distribution ratio depicted in Fig. 11*a*.

Fig. 16. Maximum story displacements of buckling-restrained brace frames designed by the proposed method: (*a*) a three-story structure, (*b*) a six-story structure, and (*c*) an eight-story structure.

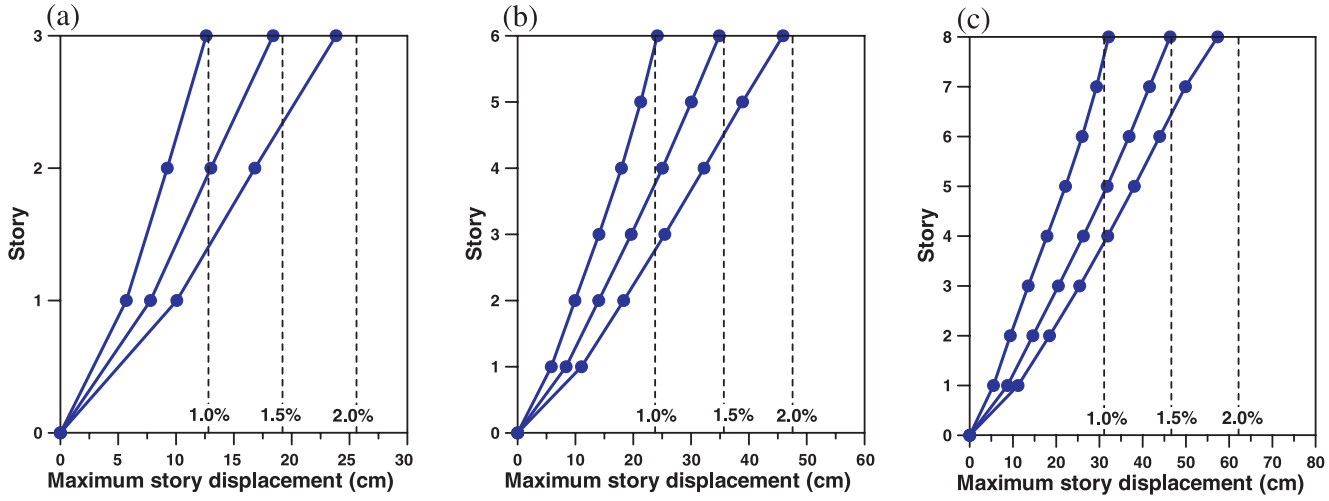

Fig. 17. Maximum inter-story drifts of buckling-restrained brace frames designed by the proposed method: (*a*) a three-story structure, (*b*) a six-story structure, and (*c*) an eight-story structure.

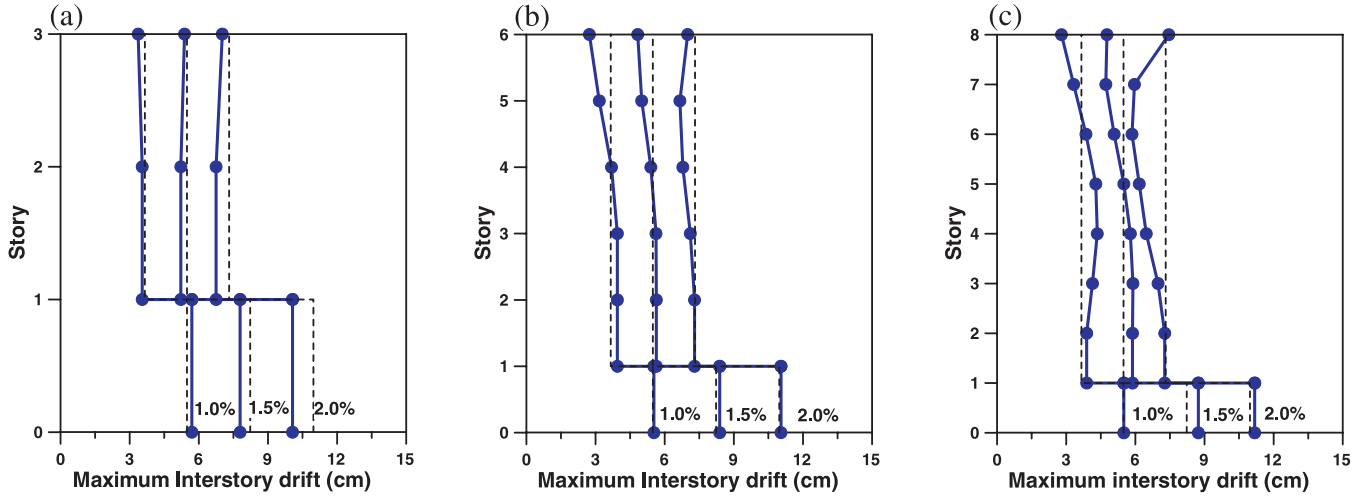

Step 6. Determination of the cross-sectional area of buckling-restrained braces (A_{bi})

The cross-sectional area of the BRBs located in a story is computed using eq. [15] in such a way that the BRB dissipates all the plastic energy distributed to the story. The first trial values for the cross-sectional area of BRBs determined in each story is: $A_{b1} = 42.2$ cm^2, $A_{b2} = 26.8$ cm^2, and $A_{b3} = 18.7$ cm^2. Then eigenvalue analysis is performed using the first-trial size of BRB to compute the next-trial value for the natural period and mode shape vector. The cross-sectional area of the BRB is refined using the newly obtained modal properties, and the process from Step 2 to Step 5 is repeated until convergence. After the fourth iteration the difference in natural period with the previous one becomes less than the 2.0%. The design process is summarized in Table 1.

Verification of the design method

The final cross-sectional area of the BRBs and the natural periods and the ductilities of the BRBF designed following the proposed design procedure are summarized in Table 2 for the three target displacements. To verify the validity of the design procedure, time-history analyses were carried out using the 20 earthquake records used previously for design. Figures 16 and 17 depict the maximum story displacements and the maximum interstory drifts of the model structures. Mean values of the analysis results are plotted in bold lines and the vertical dotted lines denote the target performance levels. According to the analysis results, the maximum story displacements and the maximum interstory drifts of the nine structures generally match well with the target displacements. Also the interstory drifts turned out to be uniform over the structure height, which is desirable in that uniform interstory drifts indicate uniform damage distribution.

Conclusions

In this study a modified energy-balance concept was applied to the seismic design of structures with buckling-restrained braces. The errors associated with the energy-balance concept

were identified and were reduced by implementing proper correction factors. According to the time-history analysis results, the behavior of the buckling-restrained braced frames designed in accordance with the proposed procedure generally coincided well with the given target performance. Compared with the seismic design based on the energy-balance concept conducted previously (Leelataviwat et al. 2002; Kim et al. 2005), the modification proposed in this study provided more precise performance-based seismic design methodology for BRBF. Although the computation of the correction factors may complicate the design and reduce the main advantage of the energy-balance concept, the procedure can be simplified if the correction factors are prepared in advance in a generalized format, such as design spectrum.

Acknowledgements

This research was supported by the Ministry of Construction & Transportation of Korea (C105A1050001-05A0505-00210), and the National Research Laboratory Program. Their financial supports are greatly acknowledged.

References

Akbas, B., Shen, J., and Hao, H. 2001. Energy approach in performance-based seismic design of steel moment resisting frames for basic safety objective. The Structural Design of Tall Buildings, **10**(3): 193–217.

ATC. 1996. Seismic evaluation and retrofit of concrete buildings. Report No. ATC-40, Applied Technology Council, Redwood City, Calif.

Black, C., Makris, N., and Aiken, I.D. 2002. Component testing, stability analysis and characterization of buckling restrained unbonded braces. Report No. PEER-2002/08, PEERC, University of California, Berkeley, Calif.

Choi, H., and Kim, J. 2006. Energy-based seismic design of buckling-restrained braced frames using hysteretic energy spectrum. Engineering Structures, **28**(2): 304–311.

Chou, C.C., and Uang, C.M. 2003. A procedure for evaluating seismic energy demand of framed structures. Earthquake Engineering and Structural Dynamics, **32**(2): 229–244.

Clark, P.W., Aiken, I.D., Kasai, K., Ko, E., and Kimura, I. 1999. Design procedure for buildings incorporating hysteretic damping devices. Proceedings of the 68th Annual SEAOC Convention, Santa Barbara, California, June 1999. Structural Engineers Association of California, Sacramento, Calif.

Dasgupta, P., Goel, S.C., Parra-Montesinos, G., and Tsai, T.C. 2004. Performance-based seismic design and behavior of a composite buckling restrained braced frame. *in* Proceedings of the 13th World Conference on Earthquake Engineering, Vancouver, B.C. 1–6 August 2004.

Decanini, L.D., and Mollaioli, F. 2001. An energy-based methodology for the assessment of seismic demand. Soil Dynamics and Earthquake Engineering, **21**(2): 113–137.

Estes, K.R., and Anderson, J.C. 2002. Hysteretic energy demands in multistory buildings. *In* Proceedings of the Seventh U.S. National Conference on Earthquake Engineering, Boston, Mass. Earthquake Engineering Research Institute, Oakland, Calif. 21–25 July 2002.

Fajfar, P., and Vidic, T. 1994. Consistent inelastic design spectra: hysteretic and input energy. Earthquake Engineering and Structures Dynamics, **23**(5): 523–537.

Housner, G. 1956. Limit design of structures to resist earthquakes. Proceedings of the First World Conference on Earthquake Engineering, Berkeley, California, June 1956. Earthquake Engineering Research Institute, San Francisco, Calif.

ICC. 2000. International building code. International Code Council, Falls Church, Va.

Khashaee, P., Mohraz, B., Lew, H.S., and Gross, J.L. 2003. Distribution of earthquake input energy in structures. Report No. NISTIR-6903, National Institute of Standards and Technology, Gaithersburg, Md.

Kim, J., Choi, H., and Chung, L. 2005. Energy-based seismic design of structures with buckling-restrained braces. Steel and Composite Structures, **4**(6): 437–452.

Leelataviwat, S., Goel, S.C., and Stojadinoviæ, B. 2002. Energy-based seismic design of structures using yield mechanism and target drift. Journal of Structural Engineering, **128**(8): 1046–1054.

Mahin, S.A., and Lin, J. 1983. Inelastic response spectra for single degree of freedom systems. Department of Civil Engineering, Univesity of California, Berkeley, Calif.

Merritt, S., Uang, C.M., and Benzoni, G. 2003. Subassemblage testing of corebrace buckling-restrained braces. Report No. TR-2003/01, University of California, San Diego, Calif.

Newmark, N.M., and Hall, W.J. 1982. Earthquake spectra and design. Earthquake Engineering Research Institute, Oakland, Calif.

SEAOC. 1995. Vision 2000, Performance-based seismic engineering of buildings. SEAOC Vision 2000 Committee, Structural Engineers Association of California, Sacramento, Calif.

Somerville, P., Smith, H., Puriyamurthala, S., and Sun, J. 1997. Development of ground motion time histories for phase 2 of the FEMA/SAC steel project. SAC Joint Venture, SAC/BD-97/04.

Tsai, K.C., and Li, J.W. 1997. DRAIN2D+: A general purpose computer program for static and dynamic analyses of inelastic 2D structures supplemented with a graphic processor. Report No. CEER/R86-07, National Taiwan University, Taipei, Taiwan.

Uang, C.M., and Bertero, V.V. 1988. Use of energy as a design criterion in earthquake-resistant design. Report No. UCB/EERC-88/18, Earthquake Engineering Research Center, University of California, Berkeley, Calif.